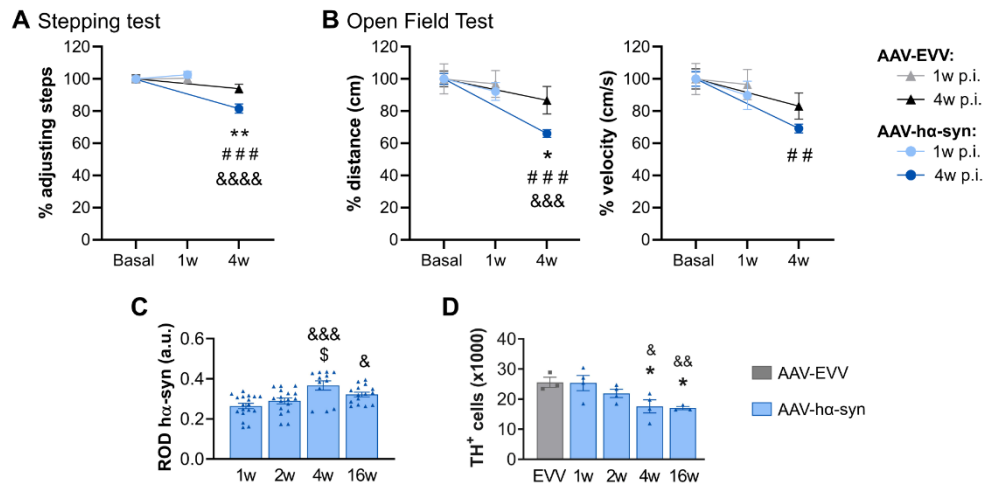# Supplementary Material

Supplementary Figures

Supplementary Figure 1. Confirmation of the animal model of experimental parkinsonism. (A) Stepping test. **(B)** Open field test. All values at each time-point were normalized to their corresponding basal values and represented as a percentage (%). The values are represented as the mean ± SEM and analyzed with a two-way ANOVA followed by a Bonferroni's *post hoc* test: [##]$P < 0.01$, [###]$P < 0.001$ vs. basal; *$P < 0.05$, **$P < 0.01$ vs. AAV-EVV; [&&&]$P < 0.001$, [&&&&]$P < 0.0001$ vs. 1 week p.i. (n = 8 for each group and time-point). **(C)** Relative optical density (ROD) analysis of hα-syn expression in the SNpc of the AAV-hα-syn rats at 1, 2, 4 and 16 weeks (w) p.i. **(D)** Quantification of TH^{+} SNpc neurons from the AAV-EVV and AAV-hα-syn rats at 1, 2, 4 and 16 weeks p.i. All values are presented as the mean ± SEM and analyzed with a Kruskal-Wallis test followed by a Dunn´s *post hoc* test: [&]$P < 0.05$, [&&]$P < 0.01$, [&&&]$P < 0.001$ vs. 1 week p.i.; [$]$P < 0.05$ vs. 2 weeks p.i.; *$P < 0.05$, vs. AAV-EVV (*n* = 4 for each group and time-point).
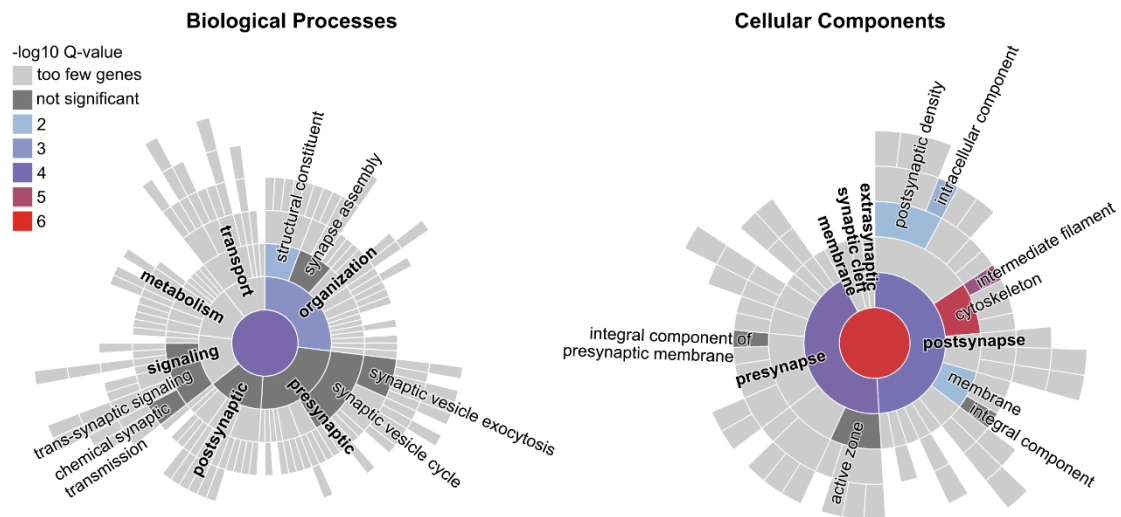
Supplementary Figure 2. Synaptic ontology analysis. Synaptic biological processes and structural components across the deregulated proteome from the AAV-hα-syn rats.
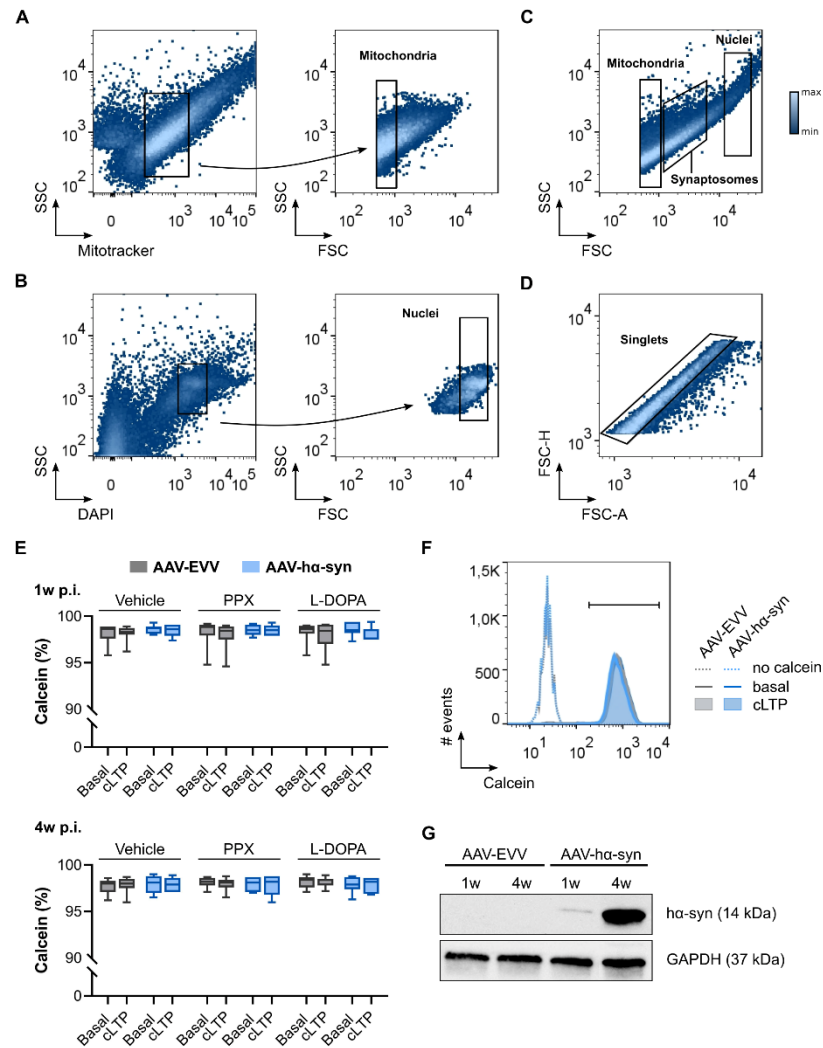
Supplementary Figure 3. Analysis of the FASS-LTP experiments. (A) Selection of the "mitochondria" size gate (~0.5 µm) based on the Mitotracker staining of isolated mitochondria. **(B)** Selection of the "nuclei" size gate (~8 µm) based on DAPI staining of isolated nuclei. **(C)** Representation of the "mitochondria" and "nuclei" size gates in synaptosomes isolated from the brain, and a selection of the "synaptosome" size gate (~0.75 to 3 µm). **(D)** Selection of single particles (singlets). **(E)** Calcein AM fluorescence (%) in synaptosomes isolated from the AAV-EVV and AAV-hα-syn animals at 1 and 4 weeks (w) p.i. at the basal state and following cLTP stimulation, when exposed to the vehicle, PPX or L-DOPA. Two-way ANOVA flowed by a Bonferroni's *post hoc* test: no significant differences were found ($n = 8$ for each group, time-point and treatment). **(F)** Representative Calcein AM staining in synaptosomes isolated from AAV-EVV and AAV-hα-syn animals in the basal state and following cLTP stimulation, and the corresponding negative controls. **(G)** Confirmation of hα-syn expression in the midbrain of AAV-EVV and AAV-hα-syn animals at 1 and 4 weeks p.i.

Supplementary Tables

Supplementary Table 1. Significant deregulated proteins in hippocampal synaptosomes in the AVV-hα-syn group

Description	Gene Name	Uniprot	Peptide Count	Ratio	P value
1 week p.i.					
Down-regulated proteins					
LETM1 domain containing 1	*Letmd1*	G3V996	2	0.3578	0.0104
Isoamyl acetate hydrolyzing esterase 1	*Iah1*	Q711G3	2	0.4028	0.0106
Formin-like 2	*Fmnl2*	A0A0G2K132	2	0.4587	0.0468
Galactosylceramidase	*Galc*	G3V6H1	2	0.5246	0.0312
Amyloid beta precursor protein	*App*	P08592	5	0.5358	0.0206
Eukaryotic translation initiation factor 3, subunit B	*Eif3b*	Q4G061	3	0.5842	0.0434
Lymphocyte cytosolic protein 1	*Lcp1*	Q5XI38	3	0.6167	0.0132
UFM1-specific peptidase 2	*Ufsp2*	Q5XIB4	4	0.6344	0.0120
Myelin oligodendrocyte glycoprotein	*Mog*	Q6MFX9	8	0.6643	0.0102
Inositol polyphosphate-4-phosphatase type I A	*Inpp4a*	D3ZBL5	10	0.6832	0.0161
Heme oxygenase 2	*Hmox2*	P23711	8	0.6918	0.0168
Myelin basic protein	*Mbp*	P02688	4	0.6924	0.0129
60S ribosomal protein L36	n.a.	D3ZZ95	3	0.6926	0.0085
PBX homeobox interacting protein 1	*Pbxip1*	A2VD12	3	0.7027	0.0482
Neurofilament medium	*Nefm*	P12839	16	0.7096	0.0125
Lymphocyte antigen 6 family member H	*Ly6h*	F1LNW6	3	0.7111	0.0002
Chloride intracellular channel 4	*Clic4*	G3V8C4	2	0.7161	0.0457
Ras homolog family member G	*Rhog*	Q32PX6	5	0.7182	0.0153
Oligodendrocytic myelin paranodal and inner loop protein	*Opalin*	Q56A26	2	0.7188	0.0016
Aminoacyl tRNA synthetase complex-interacting multifunctional protein 1	*Aimp1*	Q4G079	2	0.7188	0.0118
Carboxypeptidase M	*Cpm*	D4A9Q5	3	0.7278	0.0043
2',3'-cyclic nucleotide 3' phosphodiesterase	*Cnp*	P13233	17	0.7369	0.0025
Internexin neuronal intermediate filament protein, alpha	*Ina*	P23565	2	0.7442	0.0057
Ataxin 2-like	*Atxn2l*	B3DMA1	3	0.7543	0.0309
ATP synthase membrane subunit f	*Atp5mf*	D3ZAF6	2	0.7584	0.0412
Brain enriched myelin associated protein 1	*Bcas1*	A0A0G2K079	7	0.7606	0.0490
Serine/threonine kinase receptor associated protein	*Strap*	Q5XIG8	5	0.7617	0.0245
F-box protein 2	*Fbxo2*	G3V774	6	0.7632	0.0488
Up-regulated proteins					
Myotubularin related protein 9	*Mtmr9*	Q5XIN4	3	1.3118	0.0103
Mitogen activated protein kinase kinase 1	*Map2k1*	Q01986	2	1.3137	0.0342
Synuclein, beta	*Sncb*	A0A0G2JSQ1	4	1.3199	0.0009
Stathmin 1	*Stmn1*	P13668	2	1.3202	0.0036
Dehydrogenase/reductase 7	*Dhrs7*	D4A0T8	2	1.3214	0.0175
Microtubule-associated protein 2	*Map2*	F1LNK0	2	1.3293	0.0413
Solute carrier family 4 member 8	*Slc4a8*	F1LUB7	3	1.3336	0.0254
DnaJ heat shock protein family (Hsp40) member B12	*Dnajb12*	Q5FVC4	2	1.3358	0.0128
Poly(A) binding protein interacting protein 1	*Paip1*	D3ZZF8	2	1.3401	0.0357
Kinesin light chain 2	*Klc2*	B2GV74	6	1.3522	0.0215
Annexin A7	*Anxa7*	Q6IRJ7	11	1.3583	0.0339
Protein tyrosine phosphatase, receptor type, G	*Ptprg*	F1LP13	3	1.3724	0.0490
Solute carrier family 7, member 14	*Slc7a14*	A0A0G2K1G8	3	1.4000	0.0251
RAB6B, member RAS oncogene family	*Rab6b*	A0A0G2JT78	3	1.5058	0.0014
RAB11 binding and LisH domain, coiled-coil and HEAT repeat containing	*Relch*	D3ZJ01	7	1.5081	0.0501
Phosphofurin acidic cluster sorting protein 1	*Pacs1*	F1LPG3	13	1.5500	0.0299

Protein	Gene	Accession	#	Ratio	p-value
Tumor protein, translationally-controlled 1	*Tpt1*	P63029	2	1.6134	0.0100
Translocase of inner mitochondrial membrane 21	*Timm21*	Q5U2X7	2	1.7867	0.0203
Dispatched RND transporter family member 2	*Disp2*	D3ZBZ6	2	1.9177	0.0102
Keratin 1	*Krt1*	A0A0G2JST3	3	1.9489	0.0301
Rho GTPase activating protein 32	*Arhgap32*	F1MAK3	2	2.6862	0.0199
PiggyBac transposable element derived 5	*Pgbd5*	D3ZSZ4	2	3.0636	0.0313
Mitochondrial ribosomal protein S30	*Mrps30*	D4A833	2	3.8968	0.0138

2 weeks p.i.

Down-regulated proteins

Protein	Gene	Accession	#	Ratio	p-value
Myosin heavy chain 14	*Myh14*	F1LNF0	2	0.1059	0.0035
ZW10 interacting kinetochore protein	*Zwint*	Q8VIL3	2	0.3496	0.0387
LDL receptor related protein 1	*Lrp1*	G3V928	3	0.3845	0.0015
Mitochondrial ribosomal protein L12	*Mrpl12*	D3ZXF9	2	0.4672	0.0418
VPS33B, late endosome and lysosome associated	*Vps33b*	Q63616	3	0.4868	0.0091
Ral GTPase activating protein catalytic subunit alpha 1	*Ralgapa1*	O55007	2	0.5106	0.0051
Acyl-CoA synthetase short-chain family member 2	*Acss2*	G3V9U0	2	0.5376	0.0023
IQ motif and Sec7 domain ArfGEF 2	*Iqsec2*	A0A0G2JZX5	3	0.5455	0.0000
Phosphodiesterase 4D	*Pde4d*	A0A140TAB1	2	0.5598	0.0326
Hemoglobin subunit beta-2	n.a.	P11517	2	0.6217	0.0075
TPD52 like 2	*Tpd52l2*	Q6PCT3	3	0.6272	0.0386
Trafficking protein particle complex 3	*Trappc3*	Q5U1Z2	4	0.6340	0.0201
Synaptosome associated protein 29	*Snap29*	Q9JI56	2	0.6437	0.0118
Neurofilament heavy	*Nefh*	F1LRZ7	7	0.6553	0.0483
Hemoglobin subunit beta-2-like	*LOC103694855*	Q62669	3	0.7163	0.0308
Tropomyosin 1	*Tpm1*	A0A0G2JSQ4	2	0.7164	0.0418
VPS52 subunit of GARP complex	*Vps52*	O55166	5	0.7251	0.0026
Cytochrome c oxidase subunit 5A	*Cox5a*	P11240	6	0.7300	0.0411
Protein phosphatase 1, regulatory subunit 9A	*Ppp1r9a*	O35867	2	0.7412	0.0293
Myosin VA	*Myo5a*	A0A0G2K4Y7	17	0.7465	0.0004
Proline-rich transmembrane protein 2	*Prrt2*	D3ZFB6	3	0.7671	0.0394

Up-regulated proteins

Protein	Gene	Accession	#	Ratio	p-value
Pleckstrin and Sec7 domain containing	*Psd*	G3V8J5	6	1.3500	0.0349
Cysteine and glycine-rich protein 1	*Csrp1*	P47875	8	1.3669	0.0176
Transmembrane 9 superfamily member 4	*Tm9sf4*	A0A0G2KA25	3	1.3687	0.0113
Pleckstrin and Sec7 domain containing 3	*Psd3*	D4A2Q3	2	1.3898	0.0193
Ras homolog, mTORC1 binding	*Rheb*	Q62639	3	1.3970	0.0371
BCS1 homolog, ubiquinol-cytochrome c reductase complex chaperone	*Bcs1l*	Q5XIM0	9	1.3998	0.0103
Sodium voltage-gated channel beta subunit 1	*Scn1b*	A0A0G2JXY6	2	1.4070	0.0262
Radixin	*Rdx*	E9PT65	4	1.4076	0.0462
TAR DNA binding protein	*Tardbp*	I6L9G6	3	1.4939	0.0096
Mitochondrial ribosomal protein L10	*Mrpl10*	D3ZX69	2	1.5872	0.0449
Signal recognition particle 54A	*Srp54*	Q6AYB5	3	1.5927	0.0276
Inositol polyphosphate-4-phosphatase type I A	*Inpp4a*	D3ZBL5	7	1.7588	0.0485
Ecm29 proteasome adaptor and scaffold	*Ecpas*	F1M446	2	1.7725	0.0014
Histidyl-tRNA synthetase 1	*Hars*	Q4QQV4	2	1.9933	0.0324

4 weeks p.i.

Down-regulated proteins

Protein	Gene	Accession	#	Ratio	p-value
WD repeat domain 48	*Wdr48*	D3Z8C7	4	0.4366	0.0167
FH2 domain-containing protein	n.a.	A0A0G2JZ27	2	0.4390	0.0075
Translocase of inner mitochondrial membrane 21	*Timm21*	Q5U2X7	2	0.5102	0.0209
DIRAS family GTPase 1	*Diras1*	D4A304	2	0.5656	0.0310

Protein	Gene	Accession	Peptides	Ratio	p-value
Tubulin-folding cofactor B	*LOC103690005*	Q1RP74	2	0.5758	0.0501
Cell adhesion molecule 1	*Cadm1*	A0A5H1ZRU4	6	0.6355	0.0443
Rho GTPase activating protein 1	*Arhgap1*	D4A6C5	6	0.7576	0.0017
Up-regulated proteins					
Protein quaking-like	*LOC108348175*	F1LMH5	2	1.3592	0.0247
Phosphatidylinositol-4,5-bisphosphate 4-phosphatase 1	*Pip4p1*	Q5PPM8	2	1.4036	0.0342
UDP-glucose glycoprotein glucosyltransferase 1	*Uggt1*	Q9JLA3	9	1.4412	0.0395
Pleckstrin and Sec7 domain containing 3	*Hmgcl*	P97519	2	1.5315	0.0219
UFM1-specific peptidase 2	*Ufsp2*	Q5XIB4	3	1.5412	0.0052
Nipsnap homolog 3B	*Nipsnap3b*	Q5M949	4	1.7557	0.0201
Nucleosome assembly protein 1-like 1	*Nap1l1*	G3V6H9	3	2.1729	0.0472
Solute carrier family 25 member 23	*Slc25a23*	M0R4V4	2	2.2041	0.0402
C2 calcium-dependent domain containing 4C	*C2cd4c*	D3ZLU0	2	2.2678	0.0492
Leucine rich repeat containing 40	*Lrrc40*	G3V7I7	2	2.3373	0.0393

16 weeks p.i.

Down-regulated proteins

Protein	Gene	Accession	Peptides	Ratio	p-value
Regulator of G-protein signaling 12	*Rgs12*	G3V9H1	2	0.3423	0.0413
ATPase H+ transporting accessory protein 2	*Atp6ap2*	Q6AXS4	2	0.4141	0.0072
DExD-box helicase 39B	*Ddx39b*	Q63413	2	0.4820	0.0439
Keratin 10	*Krt10*	Q6IFW6	5	0.4894	0.0340
Glutamate metabotropic receptor 3	*Grm3*	P31422	2	0.5706	0.0477
Glutamate ionotropic receptor kainate type subunit 2	*Grik2*	P42260	3	0.6270	0.0419
ProSAAS	*LOC108348172*	G3V6X7	2	0.6508	0.0064
Calmodulin 3	*Calm3*	P0DP31	6	0.6623	0.0124
Elongator complex protein 1	*Elp1*	F1LP76	5	0.6648	0.0048
Potassium voltage-gated channel subfamily A member 1	*Kcna1*	P10499	2	0.6656	0.0350
Isoleucyl-tRNA synthetase 1	*Iars*	F1LS86	4	0.6681	0.0422
BRICK1 subunit of SCAR/WAVE actin nucleating complex	*Brk1*	D3ZUP5	2	0.6930	0.0086
Myelin basic protein	*Mbp*	P02688	4	0.6961	0.0014
Similar to RIKEN cDNA 6430548M08	*RGD1304884*	D4A3C2	4	0.7084	0.0024
Phospholipase D family, member 3	*Pld3*	Q5FVH2	4	0.7593	0.0255
Neural cell adhesion molecule 2	*Ncam2*	F1M8G9	10	0.7614	0.0483
Protein kinase cAMP-activated catalytic subunit beta	*Prkacb*	P68182	2	0.7621	0.0024
Up-regulated proteins					
Methylthioribose-1-phosphate isomerase 1	*Mri1*	Q5HZE4	2	1.3251	0.0436
Eukaryotic translation initiation factor 2 subunit gamma	*Eif2s3*	P81795	2	1.3747	0.0441
Heme binding protein 1	*Hebp1*	B4F7C7	3	1.3749	0.0422
RIMS binding protein 2	*Rimbp2*	F1LSC8	2	1.4141	0.0463
Annexin A7	*Anxa7*	Q6IRJ7	8	1.4408	0.0484
Actin related protein 10	*Actr10*	Q5M9F7	5	1.4751	0.0389
Afadin, adherens junction formation factor	*Afdn*	O35889	2	1.4871	0.0385
Microtubule affinity regulating kinase 2	*Mark2*	A0A0G2K6X6	4	1.5633	0.0027
Calpain, small subunit 1	*Capns1*	M0RD20	2	1.7931	0.0378
Brain abundant, membrane attached signal protein 1	*Basp1*	Q05175	2	2.1073	0.0212
Glutamyl-prolyl-tRNA synthetase	*Eprs*	A0A0G2JZI2	7	2.2045	0.0161

n.a. Not available

Supplementary Table 2. Synaptic ontology analysis of the functional biological processes

Ontology term	Gene Count[a]	q-value	Genes and corresponding time-points
Process in the synapse	18	8.23E-05	**1w p.i.:** SNCB, MAP2K1, INA, APP, FBXO2; **2w p.i.:** SNAP29, PRRT2, MYO5A, IQSEC2, PPP1R9A, NEFH, RHEB, PSD; **4w p.i.:** CADM1; **16w p.i:** RIMBP2, GRIK2, KCNA1, MARK2
Process in the presynapse	6	0.0130	**1w p.i.:** SNCB; **2w p.i.:** SNAP29, PRRT2; **16w p.i.:** GRIK2, KCNA1, RIMBP2
Regulation cytosolic Ca^{2+} levels			
Voltage-gated Ca^{2+} channel activity	1	n.a.	**16w p.i.:** RIMBP2
Regulation of membrane potential	2	n.a.	**16w p.i.:** GRIK2, KCNA1
Ligand-gated ion channel activity	1	n.a.	**16w p.i.:** GRIK2
Voltage-gated ion channel activity	1	n.a.	**16w p.i.:** KCNA1
Synaptic vesicle cycle	4	0.0313	**1w p.i.:** SNCB; **2w p.i.:** SNAP29, PRRT2; **16w p.i.:** RIMBP2
Regulation of synaptic vesicle cycle	1	n.a.	**2w p.i.:** SNAP29
Synaptic vesicle exocytosis	3	0.0184	**2w p.i.:** SNAP29, PRRT2; **16w p.i.:** RIMBP2
Regulation of Ca^{2+}-dependent activation of synaptic vesicle fusion	2	n.a.	**2w p.i.:** PRRT2; **16w p.i.:** RIMBP2
Regulation of synaptic vesicle exocytosis	1	n.a.	**2w p.i.:** SNAP29
Synaptic vesicle endocytosis	1	n.a.	**1w p.i.:** SNCB
Process in the postsynapse	5	0.0139	**1w p.i.:** MAP2K1; **2w p.i.:** MYO5A, IQSEC2; **16w p.i.:** GRIK2, KCNA1
Regulation of cytosolic Ca^{2+} levels	1	n.a.	**2w p.i.:** MYO5A
Regulation of membrane potential	2	n.a.	**16w p.i.:** GRIK2, KCNA1
Transmitter-gated ion channel activity	1	n.a.	**16w p.i.:** GRIK2
Voltage-gated ion channel activity	1	n.a.	**16w p.i.:** KCNA1
Regulation of membrane neurotransmitter receptor levels	2	n.a.	**1w p.i.:** MAP2K1; **2w p.i.:** IQSEC2
Synaptic signaling			
Trans-synaptic signaling	5	0.0130	**1w p.i.:** INA; **2w p.i.:** IQSEC2, PPP1R9A, NEFH; **4w p.i.:** CADM1
Retrograde signaling by trans-synaptic protein complex	1	n.a.	**4w p.i.:** CADM1
Chemical synaptic transmission	4	0.0208	**1w p.i.:** INA; **2w p.i.:** IQSEC2, PPP1R9A, NEFH
Modulation of chemical synaptic transmission	2	n.a.	**2w p.i.:** IQSEC2, PPP1R9A
Postsynaptic modulation of chemical synaptic transmission	2	n.a.	**1w p.i.:** INA; **2w p.i.:** NEFH
Synapse organization	9	8.23E-04	**1w p.i.:** INA, APP; **2w p.i.:** RHEB, NEFH, PSD, PPP1R9A; **4w p.i.:** CADM1; **16w p.i.:** MARK2, RIMBP2
Postsynapse organization	2	n.a.	**2w p.i.:** RHEB; **16w p.i.:** MARK2
Structural constituent of synapse	3	6.13E-03	**1w p.i.:** INA; **2w p.i.:** NEFH; **16w p.i.:** RIMBP2
Presynapse. Active zone	1	n.a.	**16w p.i.:** RIMBP2
Postsynapse. Postsynaptic intermediate filament cytoskeleton	2	n.a.	**1w p.i.:** INA; **2w p.i.:** NEFH

Synapse adhesion between pre- and post-synapse	1	n.a.	**4w p.i.:** CADM1
Synapse assembly	3	0.0251	**1w p.i.:** APP; **2w p.i.:** PSD; **4w p.i.:** CADM1
Presynapse assembly	1	n.a.	**4w p.i.:** CADM1
Regulation of synapse assembly	2	n.a.	**1w p.i.:** APP; **2w p.i.:** PSD
Regulation of presynapse assembly	1	n.a.	**1w p.i.:** APP
Postsynaptic specialization assembly	1	n.a.	**2w p.i.:** PSD
Maintenance of synapse structure. Postsynapse	1	n.a.	**4w p.i.:** CADM1
Postsynaptic cytoskeleton organization. Actin cytoskeleton	1	n.a.	**2w p.i.:** PPP1R9A
Metabolism			
Regulation of catabolic process modulating synaptic transmission		n.a.	
Postsynapse	1		**1w p.i.:** FBXO2
Transport		n.a.	
Establishment of ER localization to postsynapse	1		**2w p.i.:** MYO5A

[a]The gene count column shows the number of proteins that are annotated in SynGO against each term
n.a. not available

Supplementary Table 3. Synaptic ontology analysis of the structural cellular components

Ontology term	Gene Count[a]	q-value	Genes and corresponding time-points
Synapse	23	2.03E-06	**1w p.i.:** EIF3B, BCAS1, RAB6B, SNCB, NEFM, APP, INA, MAP2K1, FBXO2; **2w p.i.:** PPP1R9A, IQSEC2, VPS33B, SNAP29, PRRT2, MYO5A, NEFH, RHEB, PSD; **4w p.i.:** CADM1; **16w p.i.:** RIMBP2, KCNA1, GRM3, MARK2
Presynapse	13	7.78E-05	**1w p.i.:** RAB6B, SNCB, NEFM, APP; **2w p.i.:** PPP1R9A, IQSEC2, VPS33B, SNAP29, PRRT2; **4w p.i.:** CADM1; **16w p.i.:** RIMBP2, KCNA1, GRM3
Presynaptic cytosol	1	n.a.	**1w p.i.:** SNCB
Presynaptic cytoskeleton			
Presynaptic intermediate filament cytoskeleton	1	n.a.	**1w p.i.:** NEFM
Presynaptic active zone	3	0.0256	**1w p.i.:** APP; **2w p.i.:** IQSEC2; **16w p.i.:** RIMBP2
Presynaptic active zone cytoplasmic component	2	n.a.	**2w p.i.:** IQSEC2; **16w p.i.:** RIMBP2
Synaptic vesicle	2	n.a.	**2w p.i.:** VPS33B;SNAP29
Synaptic vesicle membrane, extrinsic component	1	n.a.	**2w p.i.:** SNAP29
Presynaptic membrane			
Integral component of presynaptic membrane	4	0.0101	**2w p.i.:** PRRT2; **4w p.i.:** CADM1; **16w p.i.:** KCNA1, GRM3
Postsynapse	14	1.30E-04	**1w p.i.:** INA, NEFM, MAP2K1, FBXO2; **2w p.i.:** MYO5A, NEFH, PPP1R9A, REHB, IQSEC2, PSD; **4w p.i.:** CADM1; **16w p.i.:** RIMBP2, KCNA1, GRM3
Postsynaptic cytoskeleton	5	4.24E-06	**1w p.i.:** INA, NEFM; **2w p.i.:** NEFH, MYO5A, PPP1R9A
Postsynaptic intermediate filament cytoskeleton	3	2.19E-05	**1w p.i.:** INA, NEFM; **2w p.i.:** NEFH
Postsynaptic actin cytoskeleton	2	n.a.	**2w p.i.:** MYO5A, PPP1R9A
Postsynaptic specialization			
Postsynaptic density	6	0.0098	**1w p.i.:** MAP2K1, INA; **2w p.i.:** PPP1R9A, RHEB, IQSEC2, PSD
Postsynaptic density intracellular component	3	0.0049	**1w p.i.:** INA; **2w p.i.:** IQSEC2, PSD
Postsynaptic density membrane	1	n.a.	**2w p.i.:** IQSEC2
Postsynaptic membrane	4	0.0098	**1w p.i.:** FBXO2; **4w p.i.:** CADM1; **16w p.i.:** KCNA1, GRM3
Extrinsic component of postsynaptic membrane	1	n.a.	**1w p.i.:** FBXO2
Integral component of postsynaptic membrane	3	0.0275	**4w p.i.:** CADM1; **16w p.i.:** KCNA1, GRM3
Postsynaptic ER			
Postsynaptic SER	1	n.a.	**2w p.i.:** MYO5A

[a]The gene count column shows the number of proteins that are annotated in SynGO against each term

Supplementary Table 4. Primary antibodies used for immunohistochemistry, immunofluorescence and flow cytometry

Antigen	Host species	Species reactivity[a]	Clone	Isotype	Dilution	Reference
α-syn	Mouse	H	Monoclonal (LB509)	IgG1k	IHC 1:500 IF 1:1000	Invitrogen, #180215
GABA	Rabbit	H, M, R	Polyclonal	IgG	IF 1:3000	GeneTex, #GTX125988
GluA1	Rabbit	M, R	Monoclonal (D4N9V)	IgG	FC 1:1500	Cell Signaling Technology, #13185S
Nrx1β	Mouse	H, M, R	Monoclonal (N170A/1)	IgG1	FC 1:400	NeuroMab, #75-216
TH	Mouse	R	Monoclonal (2/40/15)	IgG2a	IHC 1:1000	Millipore, #MAB5280
TH	Rabbit	H, M, R	Polyclonal	IgG	IF 1:1000	Merck, #AB152
vGlut2	Guinea pig	M, R	Polyclonal	IgG	IF 1:500	Synaptic Systems, #135-404

[a]We only show the following species: H, human; M, mouse; R, rat.
Abbreviations: FC, flow cytometry; IF, immunofluorescence; IHC, immunohistochemistry.

Supplementary Table 5. Secondary antibodies used for immunohistochemistry, immunofluorescence and flow cytometry

Target	Host species	Conjugate	Isotype	Dilution	Reference
Mouse	Horse	Biotinylated	IgG	IHC hα-syn 1:300 IHC TH 1:500	Vector Laboratories, #BA2000
Guinea pig	Goat	Alexa Fluor 594	IgG	IF 1:1000	Invitrogen, #A11076
Mouse	Donkey	Alexa Fluor 546	IgG	IF 1:1000	Invitrogen, #A10036
Mouse	Donkey	Alexa Fluor 647	IgG	IF 1:1000	Invitrogen, #A31571
Mouse	Goat	Alexa Fluor 647	IgG	FC 1:800	Invitrogen, #A21240
Rabbit	Goat	Alexa Fluor 488	IgG	IF 1:1000	Invitrogen, #A11034
Rabbit	Goat	Brilliant Violet 421	IgG	FC 1:400	Jackson ImmunoResearch, #111-675-144

Abbreviations: FC, flow cytometry; IF, immunofluorescence; IHC, immunohistochemistry.

Supplementary Materials and Methods

Immunohistochemistry and immunofluorescence

Immunohistochemistry

Immunohistochemistry was performed on sections containing the SNpc/VTA and the hippocampus to evaluate hα-syn expression, or the SNpc/VTA to evaluate tyrosine hydroxylase (TH) expression. Briefly, sections were washed in PBS and endogenous peroxidase activity was quenched with 3% H_2O_2 in PBS for 10 min at room temperature (RT). After several washing steps, sections were blocked with normal horse serum (NHS, 10% and 4% for hα-syn and TH, respectively) and permeabilized for 1 h at RT with Triton X-100 in PBS (PBS-T, 0.2% and 0.3% for hα-syn and TH, respectively). The sections were then incubated overnight with their corresponding primary antibodies (Supplementary Table 4) at either 4ºC for hα-syn or RT for TH. After washing in PBS, the sections were incubated with a biotinylated secondary antibody (Supplementary Table 5) for 1 h at RT followed by an avidin-biotin-peroxidase complex (1:100, Vectastain ABC kit, Vector Laboratories, #PK4000) for 1 h at RT. Finally, the signal was visualized with a 0.05% 3,3′-diaminobenzidine tetrahydrochloride (DAB; Sigma-Aldrich, #D5905)/H_2O_2 solution. All stained sections were mounted on glass superfrost slides, air-dried overnight, dehydrated in ascending alcohols, cleared in xylene, and coverslipped with the mounting medium (DPX: Panreac, #255254.1610).

Relative optical density quantification of hα-syn immunoreactivity

The extent of hα-syn expression in the SNpc/VTA and hippocampus was quantified as the relative optical density (ROD). For each animal and time point, 3 representative sections of the SNpc/VTA (approx. anteroposterior: –5.30 mm, –5.60 mm, and –6.00 mm from Bregma according to the stereotaxic atlas)[1] and hippocampus (approx. anteroposterior: -3.30 mm, -3.80 mm, and -4.16 mm from Bregma according to the stereotaxic atlas)[1] were analyzed. Images were acquired with an Aperio CS2 digital pathology slide scanner (Leica Biosystems) and the ROD values were obtained for the selected brain areas using ImageJ software (NIH) after converting the images to 8-bit greyscale images. The grey level ROD for hα-syn immunoreactivity was calculated as:

ROD = log (basal grey signal/signal grey level)[2,3]. The mean ROD values were averaged across all animals for each group and time point.

Stereological quantification of TH⁺ cells

The number of TH⁺ immunolabeled neurons was determined by stereology in regularly spaced, 50 μm thick sections that span the entire SNpc and VTA. The sections were examined on an Olympus Bx61 motorized microscope (Olympus) equipped with a DP71 digital camera (Olympus) that was connected to an XYZ stepper (H101BX, PRIOR), driven by CAST Visiopharm software (Visiopharm). The optical fractionator method was employed, using an interactive test grid controlled by the software as described previously.[4,5] A total of 7 sections per animal were quantified, covering the entire rostrocaudal extent of the SNpc and VTA (approx. anteroposterior: between -4.30 mm and -6.72 mm from Bregma according to the stereotaxic atlas).[1] TH⁺ cell bodies inside the counting frame or touching the inclusion lines were quantified. These parameters were set to reach an error coefficient below 0.10 (Gundersen, m=0) and 0.05 (Gundersen, m=1). Bilateral estimations of the TH⁺ cell populations for the SNpc and VTA were averaged across all animals for each group and time point.

Immunofluorescence

Triple immunofluorescence staining was performed on coronal free-floating sections containing the VTA to confirm the presence of hα-syn in dopaminergic (TH⁺) and glutamatergic (vGlut2⁺) neurons. Double immunofluorescent staining was also performed on coronal free-floating sections containing the hippocampus to define the dopaminergic (TH⁺), glutamatergic (vGlut2⁺), or GABAergic (GABA⁺) nature of the hα-syn⁺ fibers in the hippocampus. Briefly, sections were washed in PBS and then permeabilized for 10 min at RT in 0.3% PBS-T. After blocking with 10% normal goat serum (NGS) for 1h at RT, the sections were probed overnight at 4ºC with the corresponding primary antibodies (Supplementary Table 4) diluted in PBS. After washing with PBS, the sections were then incubated for 1 h at RT with their corresponding secondary fluorescent antibodies (Supplementary Table 5). The cell nuclei were finally counterstained for 15 min at RT with 4',6-diamidino-2-fenilindol (DAPI, 1:10,000; Invitrogen, #D1306) diluted in PBS and after washing with PBS, they were mounted on glass superfrost slides, air-dried overnight and coverslipped with Vectashield mounting medium (Vector Laboratories, # H-1400).

Confocal microscopy

Fluorescent images were acquired with a Zeiss LSM 800 laser scanning confocal microscope (Zeiss) with a Plan-Apochromat 63x/1.4 numerical aperture oil-immersion objective. Fluorescence was visualized by combining laser sets for the triple immunofluorescence of the VTA (λ = 405-488-561-633 nm) and for the double immunofluorescences of the hippocampus (λ = 405-488-561 nm). Image acquisition parameters were optimized for each marker. Images of the VTA (approx. anteroposterior: -5.30 mm from Bregma according to the stereotaxic atlas)[1] and dorsal hippocampus (approx. anteroposterior: -3.80 mm from Bregma according to the stereotaxic atlas)[1] were acquired using ZEN Imaging Software (Zeiss). The image size was 1024 x 1024 pixels with a field of view of 101.41 x 101.41 μm.

Quantitative proteomics by SWATH-MS and bioinformatics analysis

Synaptosome preparation and protein digestion

The hippocampus was rapidly dissected out and homogenized in a sucrose buffer (pH 7.4): 320 mM sucrose, 10 mM HEPES, 1 mM $MgCl_2$, 1 mM EGTA, protease inhibitors (1:1000; Sigma-Aldrich, #P8340) and phosphatase inhibitors (1:100; Thermo Fisher Scientific, #78420). The samples were centrifuged at 1,400 x g for 10 min at 4°C to obtain the supernatant (S1) containing the cytoplasm and membranous structures. To maximize sample recovery, the pellet (P1) was resuspended and centrifuged again at 800 x g for 10 min at 4°C and the S1' and S1 supernatants were mixed, while the P1' pellet was discarded. The S1/S1' mixture was centrifuged at 11,600 x g for 12 min at 4ºC, and the supernatant S2, containing the cytoplasm, was discarded and the P2 pellet, enriched in synaptosomes was resuspended in sucrose buffer. To purify the synaptosomes, resuspended samples were added on top of the same volume of a high [glucose] solution (1.4 M sucrose, 10 mM HEPES [pH 7.4] and phenol red), and centrifuged at 20,000 x g for 1 h at 4ºC to create a sucrose gradient. After centrifugation, the interphase where the synaptosomes concentrated was collected and the samples were sonicated for 10 s at medium power (Sonopuls HD2070 Bandelin), homogenized in lysis buffer (7 M urea, 2 M thiourea, and 50 mM DTT), centrifuged at 100,000 $\times$ g for 1 h at 15 °C and the protein concentration was measured with a Bradford assay (Bio-Rad). A pool of all the samples

was used as input to generate the sequential window acquisition of all theoretical mass spectra–mass spectrometry (SWATH-MS) assay library. To enhance the proteome coverage, synaptosomes were digested in-gel, and the protein extracts (30 μg) were diluted in Laemmli sample buffer and loaded into a 0.75 mm thick polyacrylamide gel with a 4% stacking gel cast over a 12.5% resolving gel. The total gel was stained with Coomassie Brilliant Blue and 12 equal slices from the pooled sample were collected from the gel. Protein enzymatic cleavage was carried out at 37 °C for 16 h with trypsin (1:20, w/w; Promega) as described previously.[6] Peptide purification and concentration was performed using C18 Zip Tip Solid Phase Extraction (Millipore), and the peptides recovered from in-gel digestion were reconstituted at a final concentration of 0.5 μg/μl in MS buffer (2% acetonitrile -ACN-, and 0.5% formic acid -FA- diluted in MilliQ-water) prior to MS analysis.

LC-MS/MS analysis to generate the spectral library

The MS/MS datasets to generate the spectral library were acquired on a TripleTOF 5600+ mass spectrometer (Sciex) associated with an Eksigent nanoLC ultra 2D pump system (Sciex) and fitted with a 75 μm ID column (0.075 × 250 mm, particle size 3 μm and pore size 100 Å; Thermo Scientific). Before separation, the peptides were concentrated on a C18 precolumn (0.1 × 50 mm, particle size 5 μm and pore size 100 Å; Thermo Scientific). The mobile phases were 0.1% FA in water (buffer A) and 0.1% FA in ACN (buffer B). Peptides were eluted in a linear gradient of buffer B from 2% to 40% over 120 min. The column was equilibrated in 95% buffer B for 10 min and 2% buffer B for 10 min. During all processes, the precolumn was in line with the column and the flow was maintained at 300 nl/min all along the gradient. The output of the separation column was directly coupled to the nano-electrospray source and the MS1 spectra were collected in the range of 350-1250 m/z for 250 ms. The 35 most intense precursors with charge states of 2 to 5 that exceeded 150 counts per second were selected for fragmentation using rolling collision energy. MS2 spectra were collected in the range of 230–1500 m/z for 100 ms and the precursor ions were dynamically excluded from reselection for 15 s.

Database search and results processing of the assay library

MS/MS data acquisition was performed using AnalystTF 1.7 (Sciex) and spectra files were processed with the ProteinPilot v5.0 search engine (Sciex) using the ParagonTM

Algorithm (v.4.0.0.0)[7] for the database search. To avoid using the same spectral evidence for more than one protein, the proteins were grouped based on MS/MS spectra using the Progroup™ Algorithm, regardless of the peptide sequence assigned. A false discovery rate (FDR) was employed using a non-linear fitting method[8] and the results displayed were those reporting a 1% Global FDR or better.

SWATH-MS

Individual protein extracts (20 μg) from all experimental groups were subjected to in-gel digestion, peptide purification and reconstitution before MS analysis, as described previously. For SWATH-MS-based experiments, the TripleTOF 5600+ instrument was configured as defined elsewhere[9], and using an isolation width of 16 Da (15 Da of optimal ion transmission efficiency and 1 Da for the window overlap), and a set of 37 overlapping windows was constructed covering the mass range 450–1000 Da. In this way, 2 μl of each sample was loaded onto a trap column (0.1 × 50 mm, particle size 5 μm and pore size 100 Å; Thermo Scientific) and desalted with 0.1% trifluoroacetic acid (TFA) at 2 μl/min for 10 min. The peptides were loaded onto an analytical column equilibrated in MS buffer (0.075 × 250 mm, particle size 3 μm and pore size 100 Å; Thermo Scientific) and peptides were eluted with a linear gradient of buffer B as described previously, infusing them onto the mass spectrometer. The Triple TOF was operated in swath mode, performing a 0.050 s TOF MS scan from 350 to 1250 m/z, followed by 0.080 s product ion scans from 230 to 1800 m/z on the 37 defined windows (3.05 s/cycle). The collision energy was set to an optimum energy for a 2+ ion at the center of each SWATH block, with a 15 eV collision energy spread.

Label-free quantitative data analysis

The resulting ProteinPilot group file from the library generated was loaded into PeakView® software (v2.1, Sciex) and peaks from the SWATH runs were extracted with a peptide threshold of 99% confidence (Unused Score ≥1.3) and a FDR <1%. As such, the MS/MS spectra of the assigned peptides were extracted by ProteinPilot and only the proteins that fulfilled the following criteria were validated: (1) peptide mass tolerance lower than 10 ppm, (2) 99% confidence in peptide identification, and (3) complete b/y ions series found in the MS/MS spectrum. Only proteins quantified with at least two unique peptides were considered.

Bioinformatics analysis

The significantly enriched structural complexes and biological processes from the proteins deregulated in the synaptosomal fractions were identified using Metascape.[10] For the generation of the different heatmaps, after the identification of all statistically enriched terms (structural complex, GO/KEGG terms; biological process, GO/KEGG terms, canonical pathways, hallmark gene sets), cumulative hypergeometric p-values and enrichment factors were calculated and used for filtering. The remaining significant terms were then hierarchically clustered into a tree based on Kappa-statistical similarities among their gene members. A 0.3 kappa score was then applied as the threshold to cast the tree into term clusters. The term with the best p-value within each cluster was selected as its representative term and displayed in a dendrogram. The heat map cells are colored by their p-values and grey cells indicate the lack of enrichment for that term in the corresponding list. The interactomes of human and rat α-syn were obtained from the curated Biological General Repository for Interaction Datasets (BioGRID: https://thebiogrid.org/).[11] The synaptic ontology analysis was performed using the SynGo platform (https://syngoportal.org/).[12] The "brain expressed" background set was selected, containing 18,035 unique genes in total, of which 1104 overlap with SynGO annotated genes. For each ontology term, a one-sided Fisher exact test was performed to compare differential datasets and the "brain expressed" background set, a result shown in the "p-value" column. To find enriched terms within the entire SynGO ontology, a multiple testing correction using the FDR was applied (q-value column).

Fluorescence analysis of single-synapse LTP (FASS-LTP)

Synaptosome isolation

The hippocampus was dissected out rapidly and homogenized on ice in a sucrose buffer (pH 7.4): 320 mM sucrose, 10 mM HEPES, protease inhibitors (1:1000; Sigma-Aldrich, #P8340) and phosphatase inhibitors (1:100; Thermo Fisher Scientific, #78420). The samples were centrifuged at 1,200 x g for 20 min at 4°C to obtain the S1 supernatant containing the cytoplasm and membranous structures, which was again centrifuged at 12,000 x g for 20 min at 4°C to obtain the S2 supernatant containing the cytoplasm and the P2 pellet enriched in synaptosomes. The S2 supernatant was discarded and P2 pellet

was resuspended in either extracellular buffer (120 mM NaCl, 3 mM KCl, 2 mM CaCl$_2$, 2 mM MgCl$_2$, 15 mM glucose, and 15 mM HEPES [pH 7.4]) or cLTP buffer (125 mM NaCl, 5 mM KCl, 2 mM CaCl$_2$, 30 mM glucose, and 10 mM HEPES [pH 7.4]). Synaptosomes in either the extracellular or cLTP buffer were incubated in a cell culture dish (30 mm) for 10-15 min at RT and transferred to flow cytometry tubes (180 μL containing 30-75 µg of synaptosomes/tube). An aliquot of each sample was used to determine the protein concentration using the BCA Assay (Thermo Fisher Scientific, #23227).

Incubation with dopaminergic drugs

Fresh stock solutions (100X) of the dopaminergic drugs PPX (1 mM; Sigma-Aldrich, #A1237) and L-DOPA (3 mM; Sigma-Aldrich, #D1507-5G) were prepared in distilled water. After P2 synaptosome isolation, 2 μL of each drug was added to the synaptosomes in both the extracellular and cLTP buffers (final [PPX] = 10 µM and [L-DOPA] = 30 µM). As a control, 2 µL of distilled water (vehicle) was added to the synaptosomes in both the extracellular and cLTP buffers. All the samples were incubated for 10 min at 37ºC.

Stimulation of cLTP

To prime NMDARs, a glycine solution (5 mM glycine, 0.01 mM strychnine and 0.2 mM bicuculline methiodide, diluted in cLTP buffer) was added to the synaptosomes in cLTP buffer. As a control, the same volume of extracellular buffer was added to the synaptosomes in extracellular buffer. All samples were incubated for 15 min at 37°C and the synaptosomes were then depolarized by adding a high [KCl] solution (50 mM NaCl, 100 mM KCl, 2 mM CaCl$_2$, 30 mM glucose, 0.5 mM glycine, 10 mM HEPES, 0.001 mM strychnine and 0.02 mM bicuculline methiodide [pH 7.4]) to the synaptosomes in cLTP buffer. As a control, the same volume of extracellular buffer was added to the synaptosomes in extracellular buffer, again incubating all the samples for 30 min at 37°C. Stimulation was stopped by adding ice-cold EDTA (0.1 mM in PBS) and blocking the samples with 5% fetal bovine serum (FBS, Gibco, #10500-064) in PBS. The tubes were chilled on ice, immediately centrifuged at 2,500 x g for 10 min at 4°C and the supernatant was discarded, while the pellet was resuspended with gentle agitation on ice.

Fluorescent staining of synaptosomes

After blocking, the resuspended synaptosomes were probed for 30 min at 4 °C with primary antibodies against GluA1 and Nrx1β (Supplementary Table 4), and Calcein AM (100 nM, eBioscience™, #65-0853-39). The samples were then washed with ice-cold 5% FBS and centrifuged at 2,500 x g for 10 min at 4°C. The supernatant was discarded, and the synaptosomes were resuspended and incubated for 30 min at 4°C with the corresponding secondary antibodies conjugated to Brilliant Violet 421 or Alexa Fluor 647 (Supplementary Table 5), respectively, and Calcein AM (100 nM) in the dark. After one last washing step with ice-cold PBS, the synaptosomes were resuspended in PBS and stored protected from light at 4°C until they were analyzed by flow cytometry.

Isolation and fluorescent labelling of mitochondria and nuclei (size-standards)

The mitochondria and nuclei isolated from rat liver were used as biological size-standards to identify synaptosomes by flow cytometry. To isolate mitochondria, rat livers were homogenized in sucrose buffer (pH 7.4): 200 mM sucrose, 10 mM Tris, 1 mM EGTA and protease inhibitor cocktail (1:1,000). The samples were centrifuged at 600 x g for 10 min at 4°C and the S1 supernatant containing the cytoplasm was collected and centrifuged again at 7,000 x g for 10 min at 4°C to obtain the P2 pellet containing membranous structures. This P2 pellet was resuspended in ice-cold sucrose buffer and centrifuged again at 7,000 x g for 10 min at 4°C to obtain the P3 pellet containing isolated mitochondria.[13]

To isolate nuclei, rat livers were homogenized in sucrose buffer (pH 7.4): 250 mM sucrose, 5 mM $MgCl_2$ and 10 mM Tris. The samples were centrifuged at 600 x g for 10 min at 4°C and the S1 supernatant containing the cytoplasm was discarded, and the P1 pellet was resuspended in ice-cold sucrose buffer and centrifuged again at 600 x g for 10 min at 4°C to obtain the P2 pellet containing the crude nuclei. The samples were resuspended in ice-cold high-concentration sucrose buffer (2 M sucrose, 1 mM $MgCl_2$ and 10 mM Tris [pH 7.4]) and centrifuged at 16,000 x g for 30 min at 4°C to obtain the P3 pellet containing isolated nuclei.[14]

For staining, isolated mitochondria and nuclei (150-200 µg) were brought to a physiological temperature, transferred to flow cytometry tubes and incubated with Mitotracker Red CMXRos (25 nM; Invitrogen, #M7512) for 30 min at 37 ℃, or with

DAPI (1:10,000; Invitrogen, #D1306) for 10 min at RT, respectively. Samples were stored protected from light at 4°C until they were analyzed by flow cytometry.

Flow cytometry

Samples were acquired using a FACSCanto II System (BD Biosciences) equipped with a 405 nm solid state diode violet laser, a 488 nm solid state blue laser and a 633 nm helium-neon red laser. Relative size and granularity were determined by forward scatter (FSC) and side scatter (SSC) properties, respectively, and the fluorescence was detected with the photomultiplier tubes (PMTs) using bandpass (BPF) and long-pass filters (LPF): Brilliant Violet 421 and DAPI PMT1 (BPF 450±50 nm); Calcein AM PMT2 (BPF 530±30 nm; LPF 502); Mitotracker Red CMXRos PMT3 (BPF 585±42 nm; LPF 556); and Alexa Fluor 647 PMT4 (BPF 660±20 nm). The FSC, SSC, and fluorescent signals were collected using logarithmic amplification. Small fragments and debris were excluded by establishing an FSC threshold (gain = 500), and a total of 50,000 size-gated particles were collected and analyzed for each sample (event rate: ~500/s).

The flow cytometry data was analyzed using FlowJo software (v10; FlowJo, LLC). First, considering the FSC and SSC parameters, synaptosomes (~0.75 to 3 µm) were selected using isolated mitochondria (~0.5 µm) and nuclei (~8 µm) as biological size standards (Supplementary Fig. 3A-C). Next, based on the FSC-H (height) and FSC-A (area) parameters, doublets and large aggregates were excluded, selecting single events (Supplementary Fig. 3D). Fluorescence gates were set based on standard immunostaining controls. The Calcein AM[+] population was selected (Supplementary Fig. 3F) and finally, individual GluA1 and Nrx1β positive populations were selected, and the "Make and Gate" Boolean analysis tool was used to evaluate the double-positive population. For a visual representation, GluA1 and Nrx1β staining was plotted on the same graph with a quad gate. The GluA1/Nrx1β double-positive events in stimulated samples were normalized to those in unstimulated basal samples to obtain the cLTP (%). To compare within different experiments, the GluA1/Nrx1β double-positive levels were normalized to those of the AAV-EVV basal state incubated with the vehicle in each experiment. An increase in the GluA1/Nrx1β double-positive population in cLTP samples was compared to the basal condition, considered indicative of cLTP.

Western blotting

We confirmed the expression of hα-syn in the midbrain of the animals used for behavioral studies and FASS-LTP experiments in western blots (Supplementary Fig. 3G). The midbrain was dissected out along with the hippocampus, immediately frozen on dry ice and stored at -80 ºC. The midbrain was slowly defrosted, homogenized in 2% SDS buffer (10 mM Tris [pH 7.4], 2% SDS, protease inhibitor cocktail [1:1000] and phosphatase inhibitor cocktail [1:100]) and sonicated for 2 min. After 20 min on ice, the homogenates were centrifuged at 4 °C (15,900 x g for 13 min), and the supernatant was collected and stored at -80 ºC. The protein concentration was measured using the BCA protein assay (Thermo Fisher Scientific, #23227), and the midbrain samples (18 µg) were mixed with 4X loading buffer (1.25 M Tris [pH 6.8], 40% glycerol, 8% SDS, 0.04% bromophenol blue and 5% 2-mercaptoethanol) and lysis buffer (25 mM HEPES [pH 7.4], 150 mM NaCl, 1% Triton X-100 and 5 mM EDTA), and denatured at 95 °C for 10 min. The proteins were resolved in 4-15% Mini-PROTEAN®TGX Stain-Free™ Protein Gels (Bio-Rad, #4568083) and transferred to PVDF membranes using the Trans-Blot Turbo RTA Mini PVDF Transfer Kit (Bio-Rad, #1704272). The membrane was cut and the lower part that corresponded to the hα-syn molecular weight was fixed in 4% paraformaldehyde for 30 min. After several washing steps in TBS with 0.1 % Tween-20, the lower and upper membrane pieces were blocked with 5% skimmed milk before incubating them overnight at 4 °C with the corresponding anti-hα-syn primary antibody (1:1,000; Invitrogen, #32-8100) or anti-GAPDH (housekeeping control: 1:10,000; Merck, #MAB374). The following day, the membranes were incubated with the corresponding HRP-conjugated secondary antibody, and signal was visualized by chemiluminescence using Immobilon Western HRP Substrate Classico (Sigma-Aldrich, #WBLUCO500) and the ChemiDoc MP system (Bio-Rad).

References for Supplementary Information

1. Paxinos G, Watson C. *The Rat Brain in Stereotaxic Coordinates, 4th Ed.*; 1998. doi:10.1017/CBO9781107415324.004

2. Tatulli G, Mitro N, Cannata SM, et al. Intermittent Fasting Applied in Combination with Rotenone Treatment Exacerbates Dopamine Neurons Degeneration in Mice. *Front Cell Neurosci*. 2018;12:4. doi:10.3389/fncel.2018.00004

3. Vermilyea SC, Guthrie S, Hernandez I, Bondarenko V, Emborg ME. α-Synuclein Expression Is Preserved in Substantia Nigra GABAergic Fibers of Young and Aged Neurotoxin-Treated Rhesus Monkeys. *Cell Transplant*. 2019;28(4):379-387. doi:10.1177/0963689719835794

4. Jiménez-Urbieta H, Gago B, Quiroga-Varela A, et al. Pramipexole-induced impulsivity in mildparkinsonian rats: a model of impulse control disorders in Parkinson's disease. *Neurobiol Aging*. 2019;75:126-135. doi:10.1016/j.neurobiolaging.2018.11.021

5. Rodríguez-Chinchilla T, Quiroga-Varela A, Molinet-Dronda F, et al. [(18)F]-DPA-714 PET as a specific in vivo marker of early microglial activation in a rat model of progressive dopaminergic degeneration. *Eur J Nucl Med Mol Imaging*. 2020;47(11):2602-2612. doi:10.1007/s00259-020-04772-4

6. Shevchenko A, Tomas H, Havlis J, Olsen J V, Mann M. In-gel digestion for mass spectrometric characterization of proteins and proteomes. *Nat Protoc*. 2006;1(6):2856-2860. doi:10.1038/nprot.2006.468

7. Shilov I V, Seymour SL, Patel AA, et al. The Paragon Algorithm, a next generation search engine that uses sequence temperature values and feature probabilities to identify peptides from tandem mass spectra. *Mol Cell Proteomics*. 2007;6(9):1638-1655. doi:10.1074/mcp.T600050-MCP200

8. Tang WH, Shilov I V, Seymour SL. Nonlinear fitting method for determining local false discovery rates from decoy database searches. *J Proteome Res*. 2008;7(9):3661-3667. doi:10.1021/pr070492f

9. Gillet LC, Navarro P, Tate S, et al. Targeted data extraction of the MS/MS spectra generated by data-independent acquisition: a new concept for consistent and

accurate proteome analysis. *Mol Cell Proteomics*. 2012;11(6):O111.016717. doi:10.1074/mcp.O111.016717

10. Zhou Y, Zhou B, Pache L, et al. Metascape provides a biologist-oriented resource for the analysis of systems-level datasets. *Nat Commun*. 2019;10(1):1523. doi:10.1038/s41467-019-09234-6

11. Oughtred R, Stark C, Breitkreutz BJ, et al. The BioGRID interaction database: 2019 update. *Nucleic Acids Res*. 2019;47(D1):D529-D541. doi:10.1093/nar/gky1079

12. Koopmans F, van Nierop P, Andres-Alonso M, et al. SynGO: An Evidence-Based, Expert-Curated Knowledge Base for the Synapse. *Neuron*. 2019;103(2):217-234.e4. doi:10.1016/j.neuron.2019.05.002

13. Frezza C, Cipolat S, Scorrano L. Organelle isolation: Functional mitochondria from mouse liver, muscle and cultured filroblasts. *Nat Protoc*. 2007;2(2):287-295. doi:10.1038/nprot.2006.478

14. Nagata T, Redman RS, Lakshman R. Isolation of intact nuclei of high purity from mouse liver. *Anal Biochem*. 2010;398(2):178-184. doi:10.1016/j.ab.2009.11.017